

Comparative experimental study of ionic polymer-metal composites with different backbone ionomers and in various cation forms

Sia Nemat-Nasser and Yongxian Wu

University of California, San Diego, Center of Excellence for Advanced Materials

9500 Gilman Drive, La Jolla, CA 92093-0416

Electronic mail: sia@ucsd.edu

An ionic polymer-metal composite (IPMC) consisting of a thin perfluorinated ionomer (usually, Nafion or Flemion) strip, platinum, and/or gold plated on both faces and neutralized by a certain amount of appropriate cations undergoes large bending motion when, in a hydrated state, a small electric field is applied across its thickness. When the same membrane is suddenly bent, a small voltage of the order of millivolts is produced across its surfaces. Hence IPMCs can serve as soft bending actuators and sensors.

This coupled electrical-chemical-mechanical response of IPMCs depends on the structure of the backbone ionic polymer, the morphology and conductivity of the metal electrodes, the nature of the cations, and the level of hydration (or other solvent uptake). We have carried out extensive experimental studies on both Nafion- and Flemion-based IPMCs in various cation forms, seeking to understand the fundamental properties of these composites, to explore the mechanism of their actuation, and finally, to optimize their performance for various potential applications. The results of some of these tests on both Nafion- and Flemion-based IPMCs with alkali-metal or alkyl-ammonium cations are reported here. Compared with Nafion-based IPMCs, Flemion-based IPMCs with fine dendritic gold electrodes have higher ion-exchange capacity, better surface conductivity, higher hydration capacity and higher longitudinal stiffness. They also display greater bending actuation under the same applied voltage. In addition, they do not display a reverse relaxation under a sustained DC voltage, which is typical of Nafion-based IPMCs in alkali-metal form. Flemion IPMCs thus are promising composites for application as bending actuators.

I. INTRODUCTION

A typical ionic polymer metal composite (IPMC) consists of a thin ionomeric membrane with noble metal electrodes plated on both its surfaces, and is neutralized with a certain amount of cations that balance the electrical charge of the anions covalently fixed to the backbone membrane. The membrane consists of perfluorinated ionomers, varying in the length and number of side chains, and in the nature of the ionic side group, usually sulfonate (Nafion[®], DuPont) or carboxylate (Flemion[®], Asahi Glass Co. Ltd.) anions.¹ Fig. 1 shows the chemical formulas of Flemion and Nafion. The metal electrodes can be platinum with a layer of finishing gold to improve surface conductivity,² like the Nafion-based IPMCs used in our tests, see Fig. 2; or they can be pure gold,³ like the Flemion-based IPMCs also used in our tests, see Fig. 3. The cations used in our study include the alkali-metal cations, Li⁺, Na⁺, K⁺, Rb⁺, and Cs⁺, as well as alkyl-ammonium cations, tetramethylammonium (TMA⁺) and tetrabutyl-ammonium (TBA⁺).

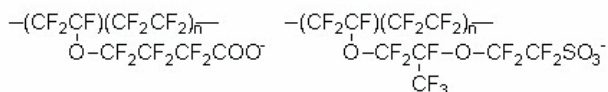


FIG. 1. Chemical formulas of Flemion (left), and Nafion (right).

II. ELECTRO-MECHANICAL RESPONSE

The electro-mechanical response (actuation) of an IPMC depends on its ionomer, counter ion, and its degree

of hydration.⁴ Different alkali-metal or alkyl-ammonium cations yield different speeds and total tip displacements for the same cantilevered strip of the IPMC.⁵

In a typical IPMC actuation test, water-saturated 3.0 by 0.3cm strips are immersed in room temperature deionized (DI) water, with one end clamped between platinum electrode grips. Then, 1 to 3V direct current (DC) is suddenly applied and maintained until the sample comes to rest, after which the voltage is removed as the two electrodes are shorted. The entire process is recorded using

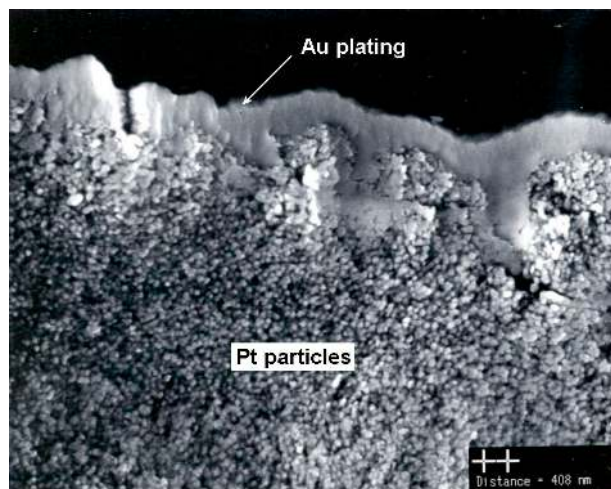


FIG. 2. Electrode morphology of Pt/Au-plated Nafion-117, showing platinum particles diffused into the Nafion membrane. The distance between two crosses is 408 nm.

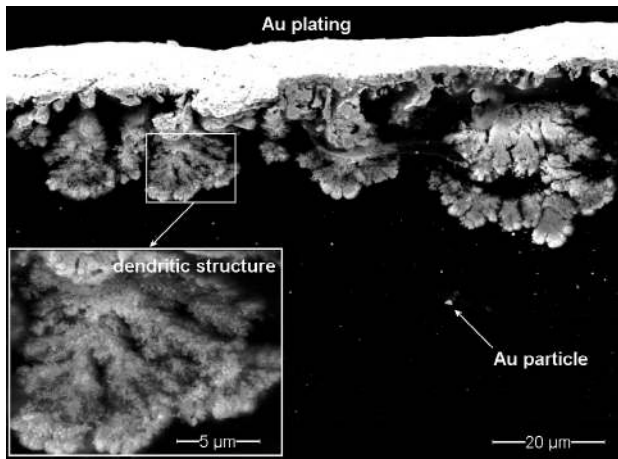


FIG. 3(a). Cross section of a typical Au-plated FLEMION-1.44, showing dendritic structure of gold electrodes with high interfacial area within the membrane;

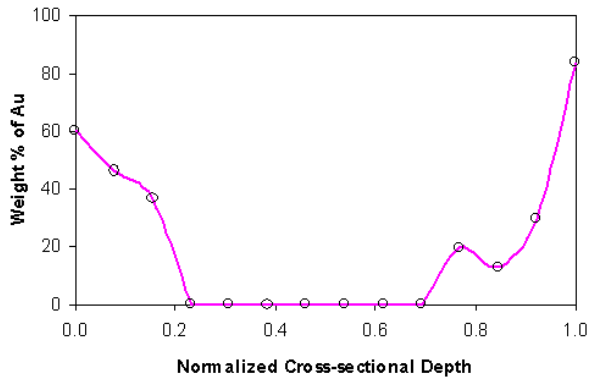


FIG. 3(b). Energy dispersive spectrometric (EDS) analysis, showing Au distribution along the cross section of an Au-plated FLEMION-1.44.

a CCD camera. A chart of normalized tip displacement (e.g., tip displacement divided by gauge length) versus time is then obtained through video analysis. Simultaneously, the current and potential across the thickness of the sample are recorded as functions of time using a Nicolet data acquisition system. The accumulated charge is obtained by the time-integration of the measured current (reduced by the residual current that continues to flow long after the actuation has ceased, due to internal resistance).

A. Actuation of Nafion-based IPMCs

When a water-saturated cantilevered strip of Nafion-based IPMC in an alkali-metal cation form is subjected to a small DC potential, it undergoes a *fast* bending deformation towards the *anode*, followed by a *slow* relaxation in the *opposite* direction (towards the cathode). If the two surfaces are shorted after the relaxation motion has stopped, the sample displays a *fast* bending deformation towards the *cathode* and then *slowly* relaxes back towards the anode, seldom attaining its initial state, see Fig. 4(a), where a Nafion-based IPMC in K⁺-form is actuated under 1V DC.

For a micromechanical analysis of IPMC actuation, see Refs. 4 and 6.

Except for some large alkyl-ammonium cations (e.g., TBA⁺), which produce a *gradual* bending towards the anode, Nafion-based IPMCs in most cation forms have an actuation behavior similar to that of Fig. 4(a), with the magnitude and speed of their displacement changing with the cation form.⁷ For TMA⁺- and Li⁺-forms, the initial fast displacement is recovered only *partially* in relaxation motion under a sustained DC voltage, whereas for Na⁺, K⁺, Rb⁺, Cs⁺, and particularly TI⁺-form, the relaxation motion takes the sample *beyond* its initial position and towards the cathode,⁸ see Fig. 4(b). We note that other actuation tests of Nafion-based IPMC in K⁺-form have shown greater back relaxation in much shorter time and much larger back displacement than that in Fig. 4.⁷

For a Nafion-based IPMC in TMA⁺-form, the magnitude of the initial fast displacement is about twice that in the alkali-metal cation form, but it has a lower speed. It takes an IPMC in TMA⁺-form up to 1.3 seconds to reach its maximum displacement, whereas the time scale of the fast motion for alkali-metal cations is a fraction of one second.

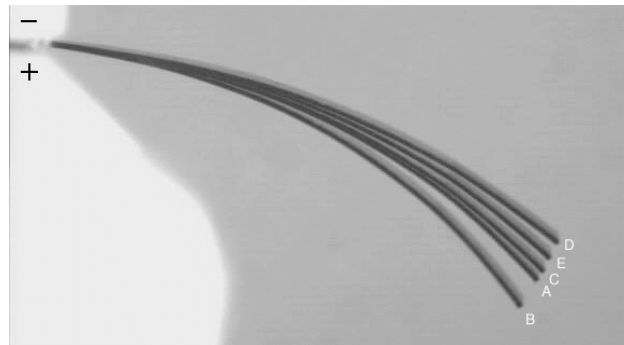


FIG. 4(a). Successive photos of actuation of a Nafion-based IPMC in K⁺-form; under 1V DC, the sample quickly (<0.1sec) bends from A to B, then slowly (>30sec) relaxes back to C, overshooting the initial position; upon shorting at C, the sample responds by a fast (<0.1sec) motion to D followed by a slow (>30sec) relaxation back to E, leaving a permanent deformation; corresponding normalized tip displacement versus time is plotted in Fig. 4(b);

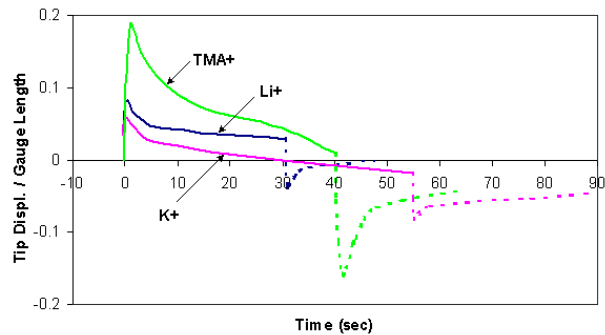


FIG. 4(b). Normalized tip displacement versus time of Nafion-based IPMCs in various cation forms. Positive displacement represents bending towards the anode; all samples are from the same IPMC sheet.

To study the IPMC's initial fast motion, a high-speed camera, Pulnix TM-6710 with 120 frames per second (FPS) scanning speed, is used. The camera is programmed for variable frame rates. Fig. 5 illustrate typical results for a Nafion-based IPMC in Na^+ -form, actuated by 1.5V DC and then shorted after about 70 seconds. The same sample is then changed into the TBA^+ -form and is actuated as before. These results are also shown in the same figures.

As is evident from the data in Figs. 5(a) and 5(b), the sample in Na^+ -form has an initial *fast* response towards the anode, followed by some vibrations due to the initial jerk, and then a *slow* back relaxation towards the cathode, *overshooting* its initial position. However, the same sample in TBA^+ -form has a *very slow* motion towards the anode, without any back relaxation. The overall displacement in this case is quite small. Fig. 5(b) shows the first 1.5 seconds after the application of the DC potential, recorded at an average 80 FPS. The zigzagged part of the displacement curve for the Na^+ -form is due to the sample vibration. The sample in TBA^+ -form has hardly moved in the first 1.5 seconds.

The current and potential across the thickness of the samples are measured during actuation, as is illustrated in Fig. 6 for a Nafion-based IPMC in Na^+ -form (not the same sample as in Fig. 5). The time-variations of the normalized displacement, current, and potential are presented in the same figure. As a potential is suddenly applied, the measured potential across the sample's two surfaces increases to and then stays at the applied voltage (1.5V). The current increases abruptly (to 108mA, in this case) and then falls to a small value (residual current of 2.3mA) gradually; this has also been observed by others.⁹ When shorted, the potential and the current have the reverse of their initial time-profiles. The potential drops to zero. The current again increases abruptly, but in the reverse direction, and then falls to a residual value.

Under DC, Nafion-based IPMCs do not maintain their initial displacement towards the anode, but rather they generally relax back towards the cathode soon after their initial fast motion and, for some cations, the back relaxation overshoots the initial position.^{8, 10} Upon shorting, a fast motion towards the cathode is followed by slow back relaxation towards the initial position, but generally leaving a permanent deformation. These facts limit the potential applications of this class of IPMCs.¹¹

B. Actuation of Flemion-based IPMCs

For Flemion-based IPMCs, a different actuation behavior is observed. When a cantilevered strip of Flemion-based IPMC in an alkali-metal cation form is actuated by an application of a DC voltage, it undergoes an initial *fast* bending towards the anode. However, unlike Nafion-based IPMCs, the sample continues to move in the *same* direction (towards the anode) but at decreasing speeds. Upon shorting, the sample has a *fast* bending motion towards the cathode, which is then followed by a slow motion in the *same* direction (towards the cathode). The results of typical tests of the same sample in Li^+ - and Na^+ -form are presented in Fig. 7, which also includes results for the same

membrane in TBA^+ -form, discussed in the sequel. In this experiment, a cantilevered strip of Flemion-based IPMC in Li^+ -form is actuated by suddenly applying 1.5V DC across its clamped end. The sample quickly bends towards the

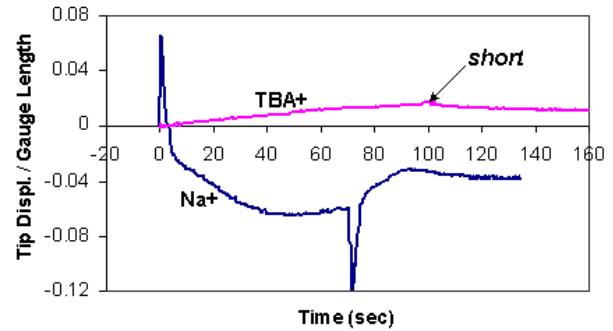


FIG. 5(a). Actuation of a Nafion-based IPMC in Na^+ - and TBA^+ -form under a 1.5V DC, applied and sustained until equilibrium is reached and then shorted; tip displacement is recorded using a high-speed camera at 80 FPS and 2 FPS for the fast and slow responses, respectively; in the Na^+ -form, the initial fast response is followed by a slow reverse relaxation, whereas in the TBA^+ -form, only a very slow response towards the anode is observed;

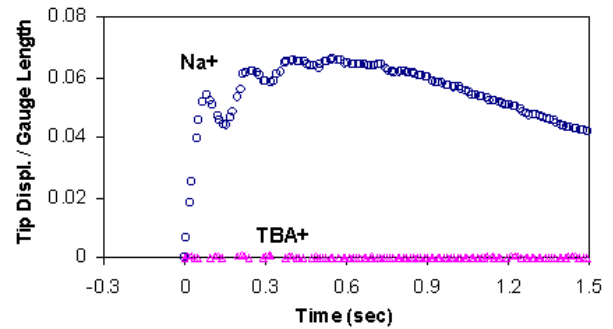


FIG. 5(b). First 1.5 seconds of actuation tests in Fig. 5(a) with (average) 80 FPS; sudden application of 1.5V DC to a Nafion-based IPMC in Na^+ -form results in a fast motion towards the anode (completed in 0.083 sec), followed by some vibration due to the initial jerk, and then slow relaxes back towards the cathode (at about 0.5 sec); a similar response is observed upon shorting; the same sample in TBA^+ -form shows very slow response towards the anode with no reverse relaxation.

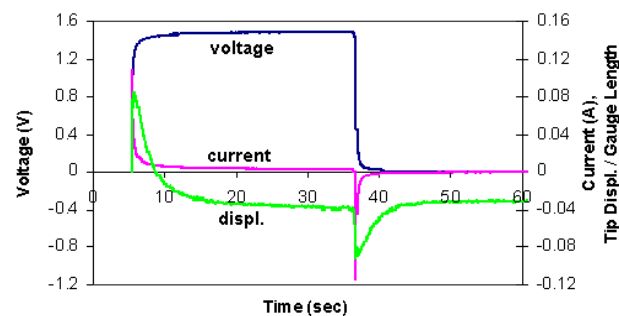


FIG. 6. Time-variation of normalized tip displacement, current, and potential for a Nafion-based IPMC in Na^+ -form, with a 1.5V DC applied and then shorted once the motion has ceased.

anode, reaching up to 77% of its total displacement in 0.125 seconds, see Fig. 7(b). After this, it moves slowly in the same direction for more than 70 seconds before essentially stopping, see Fig. 7(a). When the sample's two faces are then suddenly shorted, the sample now moves towards the cathode, first quickly and then slowly. Similar actuation behavior is observed at smaller applied potentials, e.g., 1.0V DC, which precludes possible water electrolysis.

The same sample is then changed from the Li^+ -form into the Na^+ -form, and the actuation test is repeated. With the sudden application of 1.5V DC, the sample has a fast motion towards the anode, reaching 40% of its total displacement in 0.125 seconds, followed by a slow motion in the same direction. Comparing with the Li^+ -form results, the sample in its Na^+ -form exhibits smaller maximum tip displacement in its initial fast motion and less vibration, suggesting a smaller initial internally-induced jerk in the Na^+ -form. However, its overall tip displacement is larger in the latter case due to the greater tip displacement during the slow motion.

Different actuation of IPMCs occurs with organic cations, such as tetrabutylammonium (TBA^+). For Flemion-based IPMCs with gold electrodes, large deflections can be achieved.¹² However, the displacement rate decreases with increasing cation molecular size,⁵ possibly due to a corresponding decrease in its mobility.^{13, 14} The actuation of a Flemion-based IPMC (the same strip as before) in TBA^+ -form is also shown in Fig. 7. When 1.5V DC is applied across the strip, the sample moves *continuously* and *gradually* towards the anode with decreasing speed. Compared with the other two cations, there is no detectable initial fast motion or slow relaxation in this case. In the TBA^+ -form, the sample has the largest overall tip displacement and the smallest speed.

The current and potential across the thickness of the sample are recorded during the actuation. An example is given in Fig. 8, corresponding to a Flemion-based IPMC in Na^+ -form. The tip displacement, the current, and the potential are plotted versus time. Compared with Nafion-based IPMCs, the time-variations of the current and potential are similar but occur at greater speeds (the curves have sharper slopes).

Generally, IPMCs in alkali-metal cation-form produce electrolysis under higher than a critical voltage, which is another barrier to obtaining large displacements. This undesirable electrochemical reaction consumes power and may damage the electrodes by producing gas.¹³ In our experiments, electrolysis has not been observed for Flemion-based IPMCs in TBA^+ -form, for up to 3V. Remarkably large displacements are displayed by these samples, as is illustrated in Fig. 9, where a 3V DC is applied across a Flemion-based IPMC in TBA^+ -form. The sample bends *continuously* towards the anode with decreasing speed. After 3.5 minutes, it has formed nearly a circle.

Nafion-based IPMCs in TBA^+ -form are not as active as the Flemion-based ones, having very small tip displacements and slow motion, possibly due to the smaller channels that connect the hydrophilic clusters in their

Nafion backbone matrix.^{5, 15} A basic character of TBA^+ -form IPMCs is their slow response to electric stimulus, req-

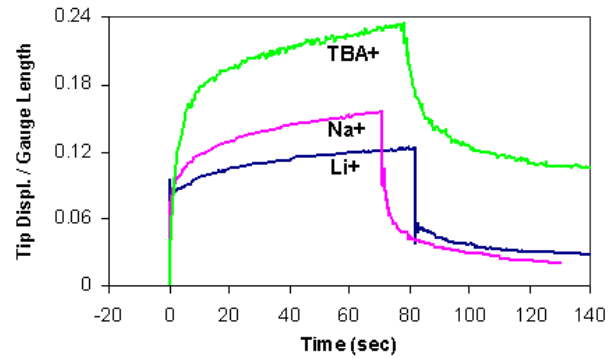


FIG. 7(a). Actuation of Flemion-based IPMC in Li^+ , Na^+ , and TBA^+ -form, under 1.5V DC, which is applied and sustained until equilibrium, and then shorted; in TBA^+ -form, it has a slow continuous gradual motion that leads to the largest overall tip displacement, whereas actuation in Li^+ - and Na^+ -form consists of an initial fast motion, followed by a slow motion, all towards the anode; there is no back relaxation;

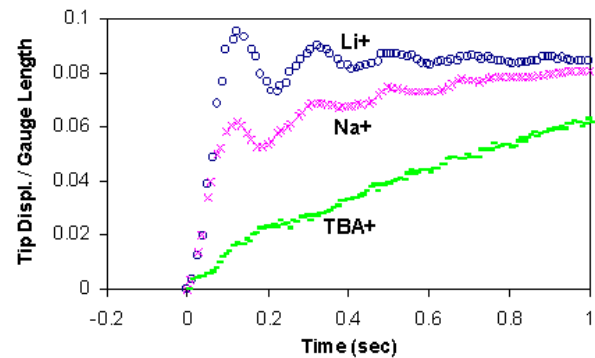


FIG. 7 (b). Tip displacement of a Flemion-based IPMC in its first 1 second of actuation in Fig. 7(a), obtained at an average of 80 FPS; in the Li^+ - and Na^+ -form, the strip has an initial fast motion, respectively reaching up to 77% and 40% of its total displacement in about 0.125 seconds and displaying vibration due to the initial jerk, while in the TBA^+ -form, it has a relatively slow and gradual motion.

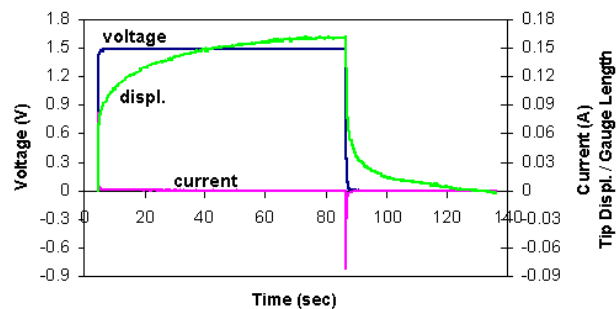


FIG. 8. Actuation test of a Flemion-based IPMC in Na^+ -form under 1.5V DC, which is applied and then shorted once the motion ceases; normalized tip displacement, current, and potential are plotted versus time.

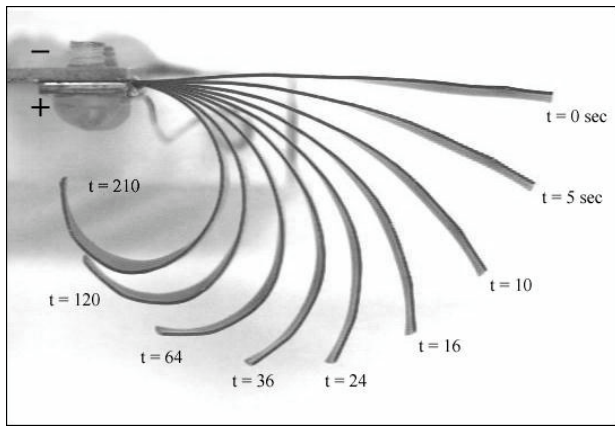


FIG. 9. Successive photos of a Flemion-based IPMC in TBA⁺-form, actuated by 3V DC; sample moves continuously towards the anode and forms nearly a circle after 3.5 minutes with no sign of electrolysis.

quiring a relatively long time to reach a certain deformation. This results in their small-amplitude vibration when actuated by a high-frequency alternating current (AC).¹⁶

C. Charge accumulation and tip displacement

The accumulated charge, representing the total charge transported by cations during actuation, is calculated by time-integration of the current, upon subtraction of the residual current (if any), which continues to flow long after the motion is essentially ceased. This value is then normalized by dividing it by the total ion capacity of the sample (or, the amount of total fixed charge, in Coulombs). For the Flemion-based IPMC sample corresponding to Fig. 8, the accumulated charge versus time is given (solid continuous curve; right Y-axis) in Fig. 10(a). The charge accumulates quickly soon after the application of the voltage, and then tends to remain constant once the sample reaches an equilibrium state with no further actuation. A total of 0.8% of the sample's fixed charge has been transported to the cathode at this equilibrium state. After the sample is shorted, the accumulated charge is reduced, again, first very quickly and then slowly, tending to a constant value. However, some of the accumulated charge may remain at the cathode, at least for a relatively long time. This is evident by the residual non-zero charge after tens of seconds in Figs. 10 and 11. In Fig. 10(a), the normalized tip displacement versus time is plotted (open circles; left Y-axis) at 30 FPS (1/30 second between adjacent points). By properly adjusting the scale of the two Y-axes (by a factor of 20 in this case), it is seen that the two curves have similar time-variations. Similar results are obtained for all other Flemion-based IPMC samples in Na⁺- and TBA⁺-forms. This suggests exploring the relation between *tip displacement* and *charge accumulation*, in an effort to explain the mechanism of IPMC actuation.⁴

In order to verify the linear relation between tip displacement and transported charge in Flemion-based IPMCs, the normalized displacement versus the correspon-

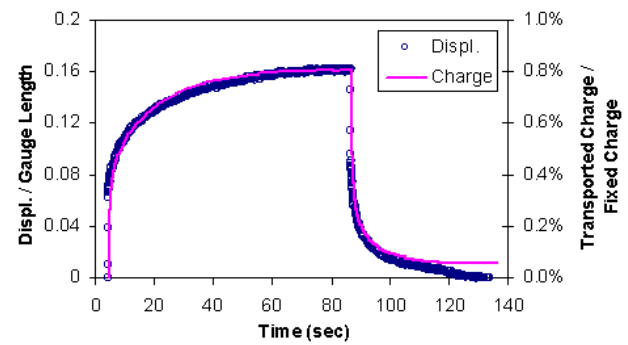


FIG. 10(a). Tip displacement and accumulated charge versus time for a Flemion-based IPMC in Na⁺-form, where 1.5V DC is applied and then shorted;

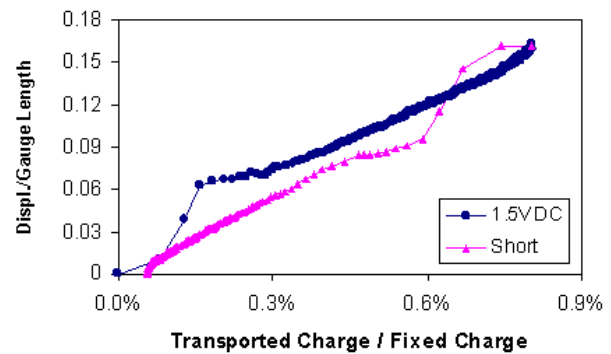


FIG. 10(b). Normalized tip displacement versus normalized accumulated charge, based on the data in Fig. 10(a).

ding value of normalized accumulated charge is plotted in Fig. 10(b). The time interval between adjacent points is 1/30 second. For both the charging (1.5V DC) and discharging (short) processes, the point density increases with time, and the relation between the normalized tip displacement and the normalized transported charge is essentially linear, with a slope of around 20. The cycle is nearly closed for the tip displacement but not for the accumulated charge. In the first 1/6 second of the charging process (the total time of charging is 86.8 seconds), up to 1/4 of the total transported charge moves to the cathode, and the sample shows a large tip displacement (2/5 of the total displacement).

Based on the test results shown in Fig. 6, and using the method outlined above, the normalized accumulated charge for the corresponding Nafion-based IPMC is calculated and plotted in Fig. 11(a). A total of 3.6% of the sample's fixed charge is transported to the cathode in this case, which is more than 4 times that of the Flemion-based IPMCs. The residual charge is considerably greater here, nearly half of the total transported charge, which corresponds to the observed permanent tip displacement after shorting; such permanent tip displacements for Nafion-based IPMCs have also been observed by others.¹⁷ The trend in charge accumulation is similar to that of the Flemion-based IPMCs. However, when comparing with the corresponding normalized tip displacement, a very different phenomenon

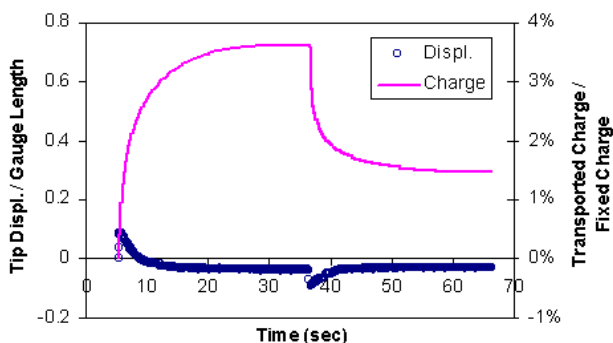


FIG. 11(a). Tip displacement and accumulated charge versus time for a Nafion-based IPMC in Na⁺-form, with 1.5V DC applied and then shorted;

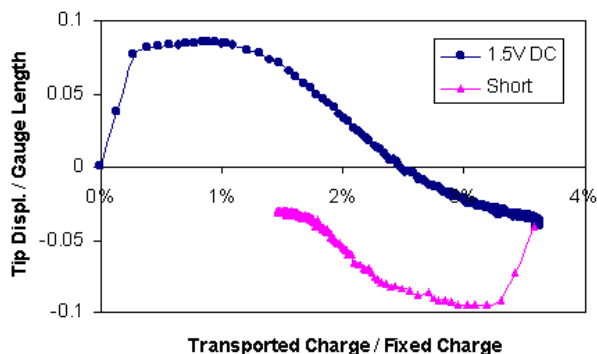


FIG. 11(b). Normalized tip displacement versus normalized accumulated charge, based on the data in Fig. 11(a).

is observed. For Nafion-based IPMCs, the initial speed of the fast displacement correlates with the speed of charge accumulation. After this fast motion, while charge transportation continues (*i.e.*, when only 26.5% of total accumulated charge has been transported), the sample begins its slow relaxation in the *opposite* direction. A similar behavior is observed during the back relaxation towards the anode, after the sample is shorted, *i.e.*, the sample continues to relax towards the anode while charges are returning to the anode side. Similar results are obtained for all other Nafion-based IPMCs in metallic cations.

The normalized tip displacement versus normalized charge accumulation for this Nafion-based IPMC is plotted in Fig. 11(b). Neither the tip displacement nor the transported charge forms a closed cycle. Again, the data points become denser in time. For the process of charging, except for the initial fast displacement towards the anode (first few points) which linearly increases with the accumulated charge, the rest of the actuation is relaxation towards the cathode despite the fact that additional cations continue to accumulate within the cathode boundary.⁴ Similar but reverse behavior is observed in the process of discharge.

III. EXPERIMENTAL DETERMINATION OF COMPOSITION

To study the micro-mechanisms of actuation, a quantitative determination of the composition of the IPMC is necessary.⁴ The mass of the polymer, the mass of the metal, and the moles of cations, as well as the amount of water uptake in each IPMC sample must be measured. The measurement of the water content is discussed separately in Section IV, in terms of the hydration volume. Here the experimental method to accurately measure other quantities is outlined.⁴

A. Ion-exchange capacity of Nafion and Flemion ionomers

The ion-exchange capacity, n , of an ionomer (*i.e.*, bare Nafion or Flemion without metal plating) is the number of moles of sulfonate or carboxylate groups within a fixed volume of material. This number corresponds to the number of moles of monovalent cations in the ionomer. The ion-exchange capacity can be determined experimentally, from the weight difference of the *same* dry ionic ionomer containing *different* cations.

If M_{A^+} and M_{B^+} are dry masses of a same ionomer sample with cations A^+ and B^+ , respectively, then

$$n = \frac{M_{A^+} - M_{B^+}}{FW_{A^+} - FW_{B^+}}, \quad (1)$$

where FW_{A^+} and FW_{B^+} are formula weights of the corresponding cation, and we have assumed monovalent cations. If more than two cations are involved, n can be obtained from the slope of the “Dry mass versus FW ” curve (see Fig. 12).

The equivalent weight (EW) of an ionomer is defined as dry mass in grams of ionic polymer in proton form divided by moles of sulfonate (or carboxylate) groups in the polymer. It is measured in grams per mole. Since the dry membrane in H⁺-form still contains some water, M_{H^+} is obtained by extrapolation. Then,

$$EW_{H^+} = \frac{M_{H^+}}{n}, \quad (2)$$

$$EW_{A^+} = EW_{H^+} - 1.008 + FW_{A^+}. \quad (3)$$

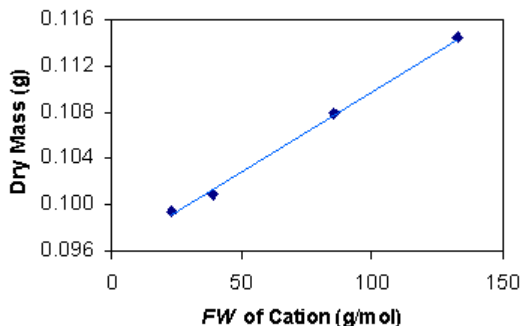


FIG. 12. Dry masses of bare Flemion-A sample in various cation forms. The results are used to determine the equivalent weight of bare Flemion ionomer.

TABLE I. Determination of equivalent weight of bare Nafion.

Quantity	Unit	Bare Nafion-A	Bare Nafion-B
M_{Na^+} ($FW_{Na^+} = 22.99$)	(g)(10^{-2})	2.217	...
M_{K^+} ($FW_{K^+} = 39.10$)	(g)(10^{-2})	...	2.183
M_{Cs^+} ($FW_{Cs^+} = 132.91$)	(g)(10^{-2})	2.428	2.364
n (slope)	(mol)(10^{-5})	1.920	1.929
M_{H^+} ($FW_{H^+} = 1.008$)	(g)(10^{-2})	2.175	2.110
EW_{H^+}	(g/mol)	1133	1093

TBABLE II. Determination of equivalent weight of bare Flemion.

Quantity	Unit	Bare Flemion-A	Bare Flemion-B
M_{Na^+} ($FW_{Na^+} = 22.99$)	(g)(10^{-1})	0.9948	0.9940
M_{K^+} ($FW_{K^+} = 39.10$)	(g)(10^{-1})	1.0099	1.0093
M_{Rb^+} ($FW_{Rb^+} = 85.47$)	(g)(10^{-1})	1.0788	1.0783
M_{Cs^+} ($FW_{Cs^+} = 132.91$)	(g)(10^{-1})	1.1445	1.1451
n (slope)	(mol)(10^{-4})	1.3884	1.4002
M_{H^+} ($FW_{H^+} = 1.008$)	(g)(10^{-1})	0.9610	0.9599
EW_{H^+}	(g/mol)	692.2	685.6

TBABLE III. Determination of metal content in Nafion-based IPMC samples.

Quantity	Unit	NF2-A	NF2-B	NF3-A	NF3-B
M_{Na^+}	(g)(10^{-2})	3.969	3.989	4.057	3.918
M_{K^+}	(g)(10^{-2})	3.998	4.022	4.087	3.939
M_{Rb^+}	(g)(10^{-2})	4.101	4.122	4.182	4.038
M_{Cs^+}	(g)(10^{-2})	4.214	...	4.309	...
n (slope)	(mol)(10^{-5})	2.243	2.135	2.284	1.968
$mass_{polymer}$	(g)(10^{-2})	2.465	2.346	2.510	2.163
$mass_{metal}$	(g)(10^{-2})	1.448	1.593	1.489	1.705
MC	%	37.0	40.4	37.2	44.1

TABLE IV. Determination of metal content in Flemion-based IPMC samples.

Quantity	Unit	FL3-A	FL3-B	FL3-C
M_{Na^+}	(g)(10^{-2})	2.989	2.864	2.850
M_{Cs^+}	(g)(10^{-2})	3.203	3.071	3.064
M_{TBA^+}	(g)(10^{-2})	3.489	3.330	3.339
n (slope)	(mol)(10^{-3})	2.278	2.123	2.228
$mass_{polymer}$	(g)(10^{-2})	1.580	1.472	1.545
$mass_{metal}$	(g)(10^{-2})	1.345	1.334	1.244
MC	%	46.0	47.5	44.6

Table I summarizes the test results for two bare Nafion samples. Sample A is changed from Na^+ - to Cs^+ -form; while sample B is changed from K^+ - to Cs^+ -form. The

measured (italic) and computed results are listed. It is known (from the manufacturer) that the equivalent weight of Nafion-117 is 1,100 g/mol. The average value in Table I is 1,113 g/mol. To refine the measurement and thus obtain a more accurate value of ion capacity, additional cations may be included, with their formula weights as far apart as possible, while avoiding strongly hydrophilic cations such as H^+ and Li^+ .

Similar measurements are performed on Flemion ionomers. Cations in two bare Flemion samples are changed from Na^+ - to K^+ - to Rb^+ - and to Cs^+ -form, sequentially. Dry masses are measured for each cation. The measured and computed results are given in Fig. 12 and Table II. The average value of equivalent weight of Flemion is obtained to be 688.9 g/mol, which is close to the reported charge density of 1.44 mequiv g^{-1} (or EW of 694.4 g/mol) for this type of Flemion ionomer.¹⁶

B. Metal content and equivalent weight of IPMC

For an IPMC, the computation must take into consideration the mass of the metal plating. First the number of moles of cations in an IPMC sample is estimated using Eq. (1) with M_{A^+} and M_{B^+} now being the corresponding dry masses of the IPMC. Then using the value of the equivalent weight of the corresponding ionomer, the mass of metal in the sample is computed,¹⁸

$$mass_{polymer} = n(EW_{H^+} - 1.008), \quad (4)$$

$$mass_{ion A^+} = n FW_{A^+}, \quad (5)$$

$$mass_{metal} = M_{A^+} - mass_{polymer} - mass_{ion A^+}. \quad (6)$$

Define the metal content of an IPMC sample, MC , measured in percent, as follows:

$$MC = \frac{mass_{metal}}{mass_{metal} + mass_{polymer}} \times 100. \quad (7)$$

The equivalent weight of the IPMC sample now is,

$$EW_{A^+} = \frac{EW_{H^+} - 1.008}{1 - MC / 100} + FW_{A^+}. \quad (8)$$

The measured dry masses of four Nafion-based IPMC samples in Li^+ -, Na^+ -, K^+ -, Rb^+ -, and Cs^+ -forms are plotted in Fig. 13. Since the sample in Li^+ -form cannot be fully dried, its measured "dry mass" does not fall on the trend line of the other cations. This is generally observed and hence the measured values are not used for the calculation of the metal content. The computational results are given in Table III. The average metal content for Nafion IPMCs used in these tests is about 40% (38.7% for NF2 and 40.7% for NF3). This value may decrease during ion exchange due to surface erosion.

Similar tests are performed on three Flemion-based IPMC samples, and the results are presented in Table IV. An average of 46.0% metal content is obtained for these samples.

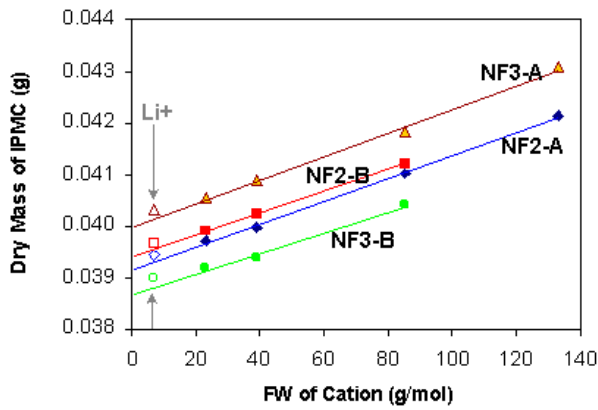


FIG. 13. Dry masses of four Nafion-based IPMC samples in various cation forms. The results are used to determine the metal content of the corresponding Nafion-based IPMC. Since the sample in Li⁺-form cannot be fully dried, its measured “dry mass” does not fall on the trend line of the other cations.

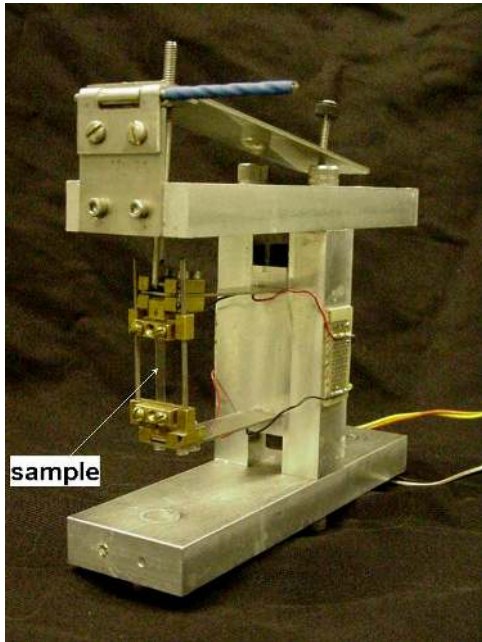


FIG. 14. Mini load frame for uniaxial extensional stiffness tests.

IV. OTHER PHYSICAL PROPERTIES OF IPMCS

A. General comments

Bare Nafion, bare Flemion, Nafion-based IPMCs, and Flemion-based IPMCs in both dry and wet form with various cations, have been studied. After ion exchange, samples are immersed in DI water for 24 hours for full hydration. Dry forms are obtained by placing the samples in a furnace at 100°C, under vacuum, for 24 hours. Results are given in Table V. Hydration is defined by the water uptake, w , which is the volume of water absorbed, V_{H_2O} , divided by the dry volume, V_{dry} , of the sample:⁴

$$w = \frac{V_{H_2O}}{V_{dry}} \tag{9}$$

For the *same* ionomer (Nafion or Flemion, with or without plating), the sample volume, mass, density, and stiffness increase with the increasing molecular weight of the cation, but the water uptake w decreases. For the same cation, a Flemion sample has smaller thickness, higher density, higher axial stiffness, and higher water uptake than a corresponding Nafion sample.

B. Stiffness versus hydration

The uniaxial extensional stiffness of bare ionomers and IPMCs is measured and presented in terms of the Young modulus. The results are used to estimate the bending stiffness of the IPMC. Our study shows that the stiffness of the bare ionomer and the IPMC is *strongly* affected by their hydration level. A dry sample may have stiffness 10 times greater than when it is water saturated. In addition, the nature of the neutralizing cation has a significant effect on the stiffness. Generally, for a same membrane at the same hydration level, the stiffness increases with increasing formula weight of the cation. The axial stiffness is measured using the mini-load frame shown in Fig. 14.

In open air, the hydration level of both dry- and wet-form samples does not remain constant. Samples in dry form absorb moisture, whereas samples in wet form lose

TABLE V. General physical properties of Nafion/Flemion ionomers and IPMCs in both dry and wet and various indicated cation forms.

			Dry Form			Water Saturated Form			
			Thickness (μm)	Density (g/cm ³)	Stiffness (MPa)	Thickness (μm)	Density (g/cm ³)	Stiffness (MPa)	Hydration Volume (%)
B A R	Nafion	Na ⁺	182.1	2.008	1432.1	219.6	1.633	80.5	71.3
		K ⁺	178.2	2.065	1555.9	207.6	1.722	124.4	50.0
		Cs ⁺	189.1	2.156	1472.2	210.5	1.836	163.6	41.4
E	Flemion	Na ⁺	149.4	2.021	2396.0	167.6	1.757	168.6	42.0
		K ⁺	148.4	2.041	2461.2	163.0	1.816	199.5	34.7
		Cs ⁺	150.7	2.186	1799.2	184.2	1.759	150.6	53.7
I P M C	Nafion-based	Cs ⁺	156.0	3.096	1539.5	195.7	2.500	140.4	54.1
	Flemion-Based	Cs ⁺	148.7	3.148	2637.3	184.1	2.413	319.0	58.1

water by evaporation. During a test, the hydration volume and thus the modulus of the sample continue to change. The cross-sectional area of the sample also changes with the hydration level, affecting the calculation of the Young modulus. These facts introduce difficulties in the stiffness measurement.

It is therefore necessary to follow a systematic experimental procedure to determine the relation between the stiffness of a strip of bare ionomer or IPMC and its hydration level. First, the dimensions and the masses of the samples are measured at the following three equilibrium states:

- (1) when the sample is water saturated (immersing the sample in DI water for at least 24 hours and keeping it in contact with water during the measurement);
- (2) when the sample attains equilibrium in open air (exposing the sample in air until its mass no longer changes); and
- (3) when the sample is nearly completely dry (drying in a furnace under vacuum for at least 24 hours and performing the measurement in an environmental chamber, in which the temperature and humidity are controlled).

These measurements are relatively easy and accurate. They yield a (linear) relation between the cross-sectional area and the hydration volume, as shown in Fig. 15(a). From this, the sample's cross-sectional area can be estimated at various hydration levels by simply measuring its weight.

Now, starting with a water-saturated sample, its stiffness is measured at various hydration levels as the sample dries in open air. The mass of the sample is measured after each stiffness measurement, and used to calculate the corresponding hydration volume and then the cross-sectional area, based on the data of Fig. 15(a). Again, starting with the same sample in dry form, its stiffness and mass are measured as its hydration level is increasing in open air. These test results now give the modulus as a function of hydration volume, as illustrated in Figs. 15(b) and 15(c).

Fig. 15 shows that Flemion samples (both bare ionomer and IPMC) have higher hydration volume and stiffness than the corresponding Nafion samples. For detailed modeling of the stiffness versus hydration, see the [Appendix](#).

C. Surface conductivity

Surface conductivity is an important electrical property governing an IPMC's actuation behavior.¹⁹ When applying a potential across the sample's thickness at the grip-end, the bending of the cantilever is affected by its surface resistance, which in turn is dependent on the electrode morphology, cation form, and the level of hydration.

A device with four platinum probes is developed to measure the IPMC's surface resistance, see Fig. 16. The voltage drop between the two inner probes and the current through the two outer probes are measured in order to calculate the IPMC's surface resistance.

Since the resistance of a sample increases with increasing length L , and decreasing width W , the specific surface resistance, R_S (in $\Omega\text{cm/cm}$), is obtained from:

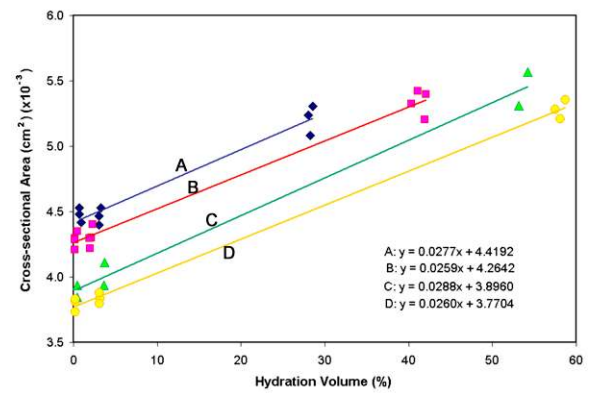


FIG. 15(a). Cross-sectional area versus hydration of Nafion/Flemion ionomers and IPMCs in Cs^+ -form, where A, B, C, and D represent Nafion-based IPMC, Nafion ionomer, Flemion ionomer, and Flemion-based IPMC, respectively;

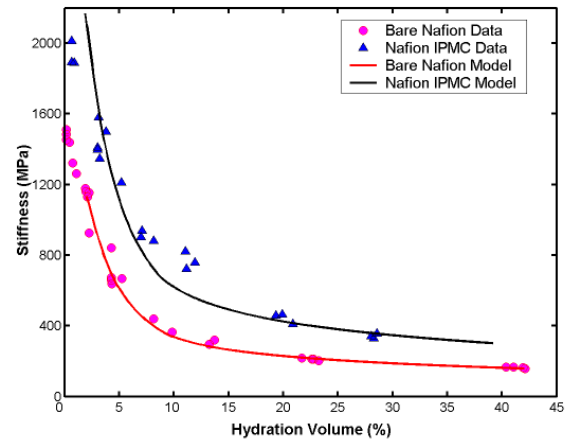


FIG. 15(b). Stiffness versus hydration of Nafion ionomer (lower data points and the solid curve) and IPMCs (upper data points and the solid curve) in Cs^+ -form;

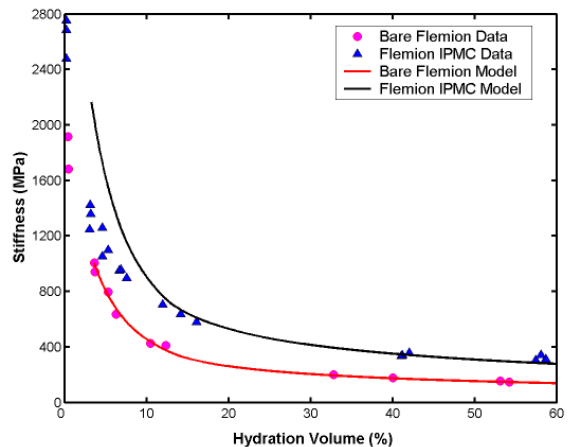


FIG. 15(c). Stiffness versus hydration of Flemion ionomer (lower data points and the solid curve) and IPMCs (upper data points and the solid curve) in Cs^+ -form. For procedures of the modeling, see [Appendix](#).

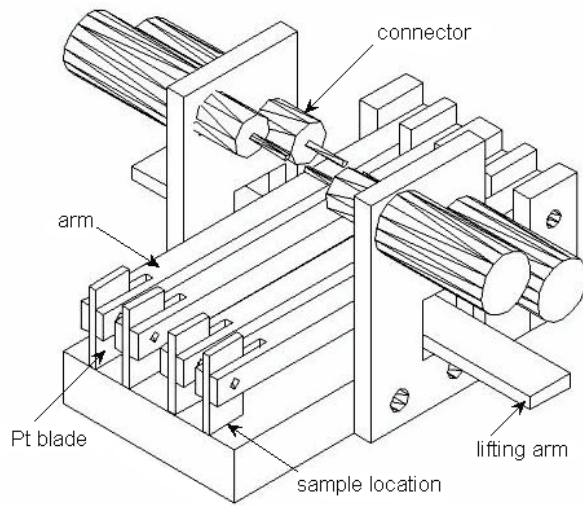


FIG. 16. A device for measuring IPMC's surface conductivity.

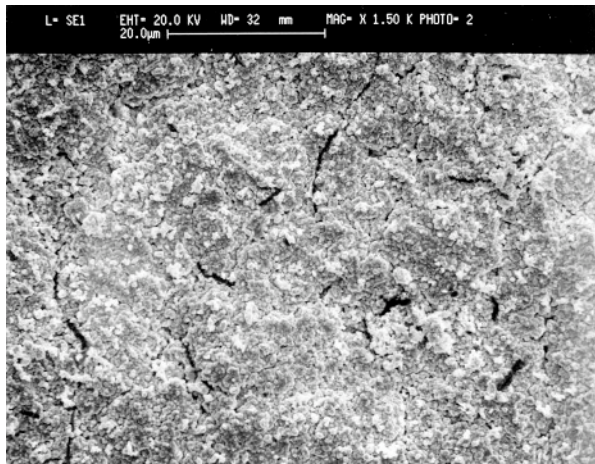
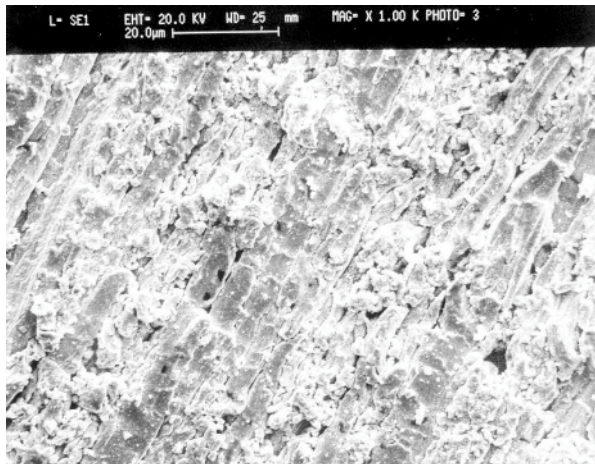


FIG. 17. Scanning electron microscopic (SEM) photos of IPMC surfaces, showing microcracks on Nafion- (upper graph) and on Flemion- (lower graph) based IPMCs.

$$R_s = R \frac{W}{L}. \quad (10)$$

Three Flemion-based and three Nafion-based IPMC samples are changed from Na^+ - to TBA^+ -form, their surface conductivity is measured in each form when water saturated, and the averages of the resulting values are given in Table VI. Generally, Flemion-based IPMCs have better surface conductivity than Nafion-based ones. The increase in specific surface resistance from the Na^+ - to the TBA^+ -form is thought to be due to the greater swelling of the ionomer in the TBA^+ -form, which expands the microcracks present in the metal electrodes, see Fig. 17.

The increase in surface resistance directly correlates with the actuation, as can be seen from the results presented in Fig. 5 and 7. In particular, the high surface resistance of the Nafion-based IPMC in the TBA^+ -form greatly hinders the corresponding actuation. To improve actuation, it is necessary to improve surface conductivity after the sample is fully hydrated and has attained its full expansion.

D. Estimated areal capacitance

An applied electric field affects the cation distribution within an IPMC membrane, forcing the cations to migrate towards the cathode. This change in the cation distribution produces two thin layers, one near the anode and another near the cathode boundaries. In time, and once an equilibrium state is attained, the anode boundary layer is essentially depleted of its cations, while the cathode boundary layer has become cation rich^{4, 8}. Let the applied constant electric potential be V and denote by Q the corresponding total charge that is accumulated within the cathode boundary layer once the equilibrium state is attained. We define the *effective electric capacitance* of the IPMC by

$$C = Q / V \quad (11)$$

and obtain the corresponding areal capacitance, measured in mF/cm^2 , by dividing by the area of the sample. Nemat-Nasser⁴ has shown that this areal capacitance has a major effect on the actuation of the corresponding IPMC.

In the actuation tests described in the preceding sections, the total equilibrium accumulated charge has been calculated by time-integration of the net current (measured current less the residual). Using the measured dimensions of each sample in saturated form, the areal capacitance is calculated and presented in Table VII. The residual current is defined by the value of current when the actuation is essentially completed.

For small alkali-metal cations such as Na^+ , Nafion-based IPMCs have larger capacitance than Flemion-based ones, using the integrated net current, as discussed above. When the ion is changed into TBA^+ , this calculated effective capacitance of Nafion-based IPMCs decreases markedly. However, this is not the case for Flemion-based IPMCs. This fact directly correlates with the observed actuation in TBA^+ -form.

TABLE VI. Specific surface resistance of Flemion- and Nafion-based IPMCs in Na⁺- and TBA⁺-form.

	R _s in Na ⁺ -form (Ωcm/cm)	R _s in TBA ⁺ -form (Ωcm/cm)
Flemion-based IPMC	0.43	1.37
Nafion-based IPMC	1.85	29.31

TABLE VII. Estimated areal capacitance of Flemion- and Nafion-based IPMCs in Na⁺- and TBA⁺-form.

	Na ⁺ -form (mF/cm ²)	TBA ⁺ -form (mF/cm ²)
Flemion-based IPMC	17.72	10.31
Nafion-based IPMC	43.24	0.34

V. SUMMARY AND CONCLUSIONS

The electro-mechanical response of an IPMC depends on its ionomer, electrodes' morphology, counter ion, and its degree of hydration. Flemion ionomers with carboxylate side groups have higher ion exchange capacity, higher stiffness, and greater water uptake than Nafion ionomers. In Pt/Au plated Nafion-based IPMCs, platinum particles deeply diffuse into the perfluorosulfonic membrane. The electrodes in Au plated Flemion-based IPMCs have a fine dendritic structure with high interfacial area, ideal for enhancing the IPMC's actuation through better surface conductivity.

The Flemion-based IPMCs in alkali-metal cation form have an initial fast bending towards the anode, followed by a slow motion in the same direction. Their actuation is directly related to the charge accumulation (defined as the integrated net current). The Nafion-based IPMCs in alkali-metal cation form have an initial fast bending towards the anode, followed by a slow relaxation in the opposite direction towards the cathode while charges continue to accumulate within their cathode boundary layer.

Different alkali-metal or alkyl-ammonium cations yield different actuation speeds and total tip displacements for the same cantilevered strip of the IPMC. Among IPMCs we tested, the Flemion-based ones in TBA⁺-form show greatest tip displacement without back relaxation. They seem to suppress water electrolysis at relatively high voltages in an aqueous environment. Their response to an electric stimulus is slow.

ACKNOWLEDGMENTS

We wish to thank Drs. Steve Wax (DARPA), Len Buckley (NRL), Carlos Sanday (NRL), and Randy Sands for their continued encouragement and many stimulating discussions; Professor Mohsen Shahinpoor and Dr. Kwang J. Kim for providing the Nafion-based IPMC samples; Dr. Kinji Asaka for providing the Flemion-based IPMC samples; Dr. Yosi Bar-Cohen for his continued interest and stimulating interaction; Professor Yitzhak Tor for comments and guidance; Mr. Jon Isaacs for developing the experimental equipment and techniques; Mr. Dave Lischer

for help in data collection, and Mr. Sai Sarva for producing Fig. 3. This work has been supported by DARPA grant number MDA972-00-1-0004 to the University of California, San Diego.

APPENDIX: STIFFNESS MODELING

A micromechanical model to estimate the stiffness of both bare and IPMC membranes as functions of the water uptake has been given by Nemat-Nasser (2002).⁴ A brief summary is presented here and results are applied to predict the stiffness versus hydration of the bare Nafion, Nafion-based IPMC, bare Flemion, and Flemion-based IPMC, in Cs⁺-form.

A. Stiffness of bare ionomer versus hydration

It is assumed that a dry sample of a bare or an IPMC membrane in an aqueous environment absorbs water until the resulting pressure within its clusters are balanced by the elastic stresses that are consequently developed within its backbone membrane. From this, the stiffness of the membrane can be calculated as a function of the water uptake for various cations. First the stiffness of the bare polymer is obtained, and then the results are used to calculate the stiffness of the corresponding IPMC by including the effect of metal electrodes.

For the backbone polymer, a neo-Hookean model is used, with the principle stresses, σ_I , related to the principal stretches, λ_I , by

$$\sigma_I = -p_0 + K\lambda_I^2, \quad (\text{A1})$$

where p_0 is an undetermined pressure to be calculated from the boundary data; in spherical coordinates, $I = r, \theta, \varphi$, for the radial and the two hoop components; and K is an effective stiffness which depends on the cation type and its concentration, and on the water uptake, w .

As a model, consider a spherical cavity of initial (*i.e.*, dry state) radius a_0 , embedded at the center of a spherical matrix of initial radius R_0 , and placed in a homogenized hydrated membrane, referred to as the *matrix*. Assume that the stiffness of both the spherical shell and homogenized matrix is the same as that of the overall effective stiffness of the hydrated membrane, which we wish to calculate. Using incompressibility, Nemat-Nasser⁴ shows that

$$\sigma_r(r_0) = -p_0 + K \left[\left(r_0/a_0 \right)^{-3} (w/w_0 - 1) + 1 \right]^{-4/3},$$

$$\sigma_\theta(r_0) = \sigma_\varphi(r_0) = -p_0 + K \left[\left(r_0/a_0 \right)^{-3} (w/w_0 - 1) + 1 \right]^{2/3}, \quad (\text{A2})$$

where r_0 measures distance from the center of sphere (Lagrangian coordinate), $w_0 = n_0/(1 - n_0)$ is the volume

fraction of the clusters in the dry condition, and n_0 is the initial porosity (volume of voids divided by total volume). The radial stress, σ_r , must equal the pressure, p_c , in the cluster, at $r_0 = a_0$,

$$\sigma_r(a_0) = -p_c. \quad (\text{A3})$$

In addition, the volume average of the stress tensor, taken over the entire membrane, must vanish in the absence of any externally applied loads. This yields a *consistency condition*,

$$\frac{1}{V_{dry}} \int_{V_{dry}} \frac{1}{3} (\sigma_r + 2\sigma_\theta) dV_{dry} - wp_c = 0. \quad (\text{A4})$$

For the hydrated bare membrane in M^+ -ion form, and in the absence of an applied electric field, the pressure within each cluster, p_c , is the sum of an osmotic, $\Pi(M^+)$, and an electrostatic, p_{DD} , component, the latter being produced by the ionic interaction that may be represented by dipole-dipole interaction forces. Detailed calculations of these two components are given by Nemat-Nasser.⁴ The final expression is:

$$p_c = \frac{2\rho_B RT\phi}{EW_{ion}w} + \frac{1}{3\kappa_e} \left(\frac{\rho_B F}{EW_{ion}} \right)^2 \frac{\pm\alpha^2}{w^2}, \quad (\text{A5})$$

where F is Faraday's constant (96,487 C/mol), ρ_B is the dry density of the bare membrane, $R = 8.31$ J/mol/K is the gas constant, $T = 300$ K is the test temperature, EW_{ion} is the equivalent weight of bare membrane, $\kappa_e = \kappa_e(w)$ is the effective electric permittivity in the cluster, $\alpha = \alpha(w)$ is an effective dipole length, and ϕ is the osmotic coefficient. From Eqs. (A3) to (A5), we obtain

$$K(w) = p_c \frac{(1+w)}{w_0 I_n - \left(\frac{w_0}{w}\right)^{4/3}},$$

$$I_n = \frac{1+2An_0}{n_0(1+An_0)^{1/3}} - \frac{1+2A}{(1+A)^{1/3}}, \quad A = \frac{w}{w_0} - 1,$$

$$p_0(w) = K \left(\frac{w}{w_0} \right)^{-4/3} + p_c. \quad (\text{A6})$$

As part of the hydration shell of an ion, water has a dielectric constant of 6, whereas as free molecules, its dielectric constant is about 78 at room temperature. The number of mole water per mole ion within a cluster is,

$$m_w = \frac{EW_{ion}w}{36\rho_B}. \quad (\text{A7})$$

Hence, when the water uptake is less than CN moles per mole of ion within a cluster, we set $\kappa_e = 6\kappa_0$, where $\kappa_0 = 8.85 \times 10^{-12}$ F/m is the electric permittivity of the free space and CN is the coordination number (number of water molecules per ion in bulk). On the other hand, when more water is available in a cluster, *i.e.*, when $m_w > CN$, we calculate κ_e as follows:⁴

$$\kappa_e = \frac{7+6f}{7-6f} 6\kappa_0, \quad f = \frac{m_w - CN}{m_w}. \quad (\text{A8})$$

We assume α^2 is linear in w for $m_w \leq CN$,

$$\pm\alpha^2 = a_1 w + a_2, \quad (\text{A9})$$

and estimate a_1 and a_2 from the experimental data. For $m_w > CN$, we assume that the distance between the two charges forming a pseudo-dipole is controlled by the effective electric permittivity of their environment (*i.e.*, water molecules), and set (measured in meter)

$$\alpha = 10^{-10} \frac{7+6f}{7-6f} (a_1 w + a_2)^{1/2}. \quad (\text{A10})$$

Fig. 15(b) shows the experimentally measured Young modulus of the bare Nafion-117 and the corresponding IPMC, in Cs^+ -form. The Young modulus Y_B of the hydrated strip of bare polymer relates to the stiffness K , by $Y_B = 3K$, based on incompressibility. The lower solid curve (bare Nafion) is obtained from Eq.(A6), using the following parameters: $FW_{\text{Cs}^+} = 132.91$ g/mol, $\rho_B = 2.16$ g/cm³ (measured dry density), $n_0 = 0.01$, and $\phi = 1$. The values of a_1 and a_2 in Eq.(A9) are obtained as 1.6383×10^{-20} and -0.0807×10^{-20} (in m²), respectively, by setting $Y_B = 1130$ MPa for $w = 0.02$ and $Y_B = 158$ MPa for $w = 0.42$. Fig. 15(c) shows the experimentally measured Young modulus of the bare Flemion-1.44 and the corresponding IPMC in Cs^+ -form. The model results (lower solid curve), are obtained based on: $EW_{H^+} = 694.4$ g/mol, $\rho_B = 2.19$ g/cm³, and $a_1 = 0.8157 \times 10^{-20}$ and $a_2 = -0.0606 \times 10^{-20}$, obtained by setting $Y_B = 1006$ MPa for $w = 0.036$ and $Y_B = 147$ MPa for $w = 0.54$.

B. Stiffness of IPMC versus hydration

To include the effect of metal plating, assume a uniaxial stress state and by volume averaging, obtaining,²⁰

$$\bar{\epsilon}_{IPMC} = f_{MH} \bar{\epsilon}_M + (1 - f_{MH}) \bar{\epsilon}_B,$$

$$\bar{\sigma}_{IPMC} = f_{MH} \bar{\sigma}_M + (1 - f_{MH}) \bar{\sigma}_B, \quad f_{MH} = \frac{f_M}{1+w}, \quad (\text{A11})$$

where the barred quantities are the average uniaxial values of the strain and stress in the IPMC, metal, and bare polymer, respectively, and f_M is the volume fraction of the metal plating in a dry sample, given by

$$f_M = \frac{(1-SF)\rho_B}{(1-SF)\rho_B + SF\rho_M}, \quad (\text{A12})$$

where ρ_M is the mass density of the metal plating and SF is the scaling factor, representing the weight fraction of dry polymer in the IPMC. The average stress in the bare polymer and in the metal are assumed to relate to the overall average stress of the IPMC, by

$$\bar{\sigma}_B = A_B \bar{\sigma}_{IPMC}, \quad \bar{\sigma}_M = A_M \bar{\sigma}_{IPMC}, \quad (\text{A13})$$

where A_B and A_M are the concentration factors. Setting $\bar{\sigma}_B = Y_B \bar{\epsilon}_B$, $\bar{\sigma}_M = Y_M \bar{\epsilon}_M$, and $\bar{\sigma}_{IPMC} = Y_{IPMC} \bar{\epsilon}_{IPMC}$, we now have

$$\bar{Y}_{IPMC} = \frac{Y_M Y_B}{BA_B Y_M + (1-BA_B) Y_B},$$

$$B = \frac{(1+\bar{w})(1-f_M)}{1+\bar{w}(1-f_M)}, \quad w = \bar{w}(1-f_M). \quad (\text{A14})$$

Here Y_B is evaluated at hydration of \bar{w} when the hydration of the IPMC is w . The latter is measured directly at various hydration levels.

The result for the Nafion-based IPMC is shown in Fig. 15(b) (upper solid curve). From Table III, the scale factor is $SF = 1 - 0.407 = 0.593 \approx 0.6$, and we set $\rho_M = 20 \text{ g/cm}^3$, for the combined overall density of gold and platinum. For Y_M we have used 75 GPa (the results are insensitive to this quantity) and for A_B we have used 0.55. For the Flemion-based IPMC, we have followed the same procedure and with $SF = 1 - 0.46 = 0.54$ (Table IV), $\rho_M = 19.3 \text{ g/cm}^3$ (for gold), $Y_M = 75 \text{ GPa}$, and for $A_B = 0.5$, have obtained the results given in Fig. 15(c) by the upper solid curve.

REFERENCE

- Carla Heitner-Wirguin, "Recent Advances in Perfluorinated Ionomer Membranes – Structure, Properties and Applications," *J. Membrane Science*, **120**, 1-33 (1996).
- Mohsen Shahinpoor and Kwang J. Kim, "Ionic Polymer-metal Composites: I. Fundamentals," *Smart Mater. Struct.*, **10**, 819-833 (2001).
- Kazuo Onishi, Shingo Sewa, Kinji Asaka, Naoko Fujiwara, and Keisuke Oguro, "Morphology of Electrodes and Bending Response of the Polymer Electrolyte Actuator," *Electrochimica Acta*, **46**, 737-743 (2000).
- Sia Nemat-Nasser, "Micro-mechanics of Ionic Polymer-metal Composites," *J. Appl. Phys.*, **92**, 2899-2915 (2002).
- Kazuo Onishi, Shingo Sewa, Kinji Asaka, Naoko Fujiwara, and Keisuke Oguro, "The Effects of Counter Ions on Characterization and Performance of a Solid Polymer Electrolyte Actuator," *Electrochimica Acta*, **46**, 1233-1241 (2001).
- Sia Nemat-Nasser and Jiang Yu Li, "Electromechanical Response of Ionic Polymer-metal Composites," *J. Appl. Phys.*, **87**, 3321-3331 (2000).
- Jeffrey McGee, "Mechano-electrochemical Response of Ionic Polymer-metal Composites," *Ph.D. Dissertation*, University of California, San Diego, (2002).
- Sia Nemat-Nasser and Chris Thomas, in *Electroactive Polymer (EAP) Actuators as Artificial Muscles - Reality, Potential and Challenges*, edited by Yoseph Bar-Cohen (SPIE, Bellingham, WA, 2001), Chap. 6, p.139-191.
- Naoko Fujiwara, Kinji Asaka, Yasuo Nishimura, Keisuke Oguro, and Eiichi Torikai, "Preparation of Gold-solid Polymer Electrolyte Composites as Electric Stimuli-responsive Materials," *Chem. Mater.*, **12**, 1750-1754 (2000).
- Kiran Mallavarapu and Donald J. Leo, "Feedback Control of the Bending Response of Ionic Polymer Actuator," *Journal of Intelligent Material Systems and Structures*, **12**, 143-155 (2001).
- Yoseph Bar-Cohen, Sean P. Leary, Andre Yavrouian, Keisuke Oguro, Satoshi Tadokoro, Joycelyn S. Harrison, Joseph G. Smith and Ji Su, "Challenges to the Application of IPMC as Actuators of Planetary Mechanisms," *Proc. SPIE*, **3987**, 140-146 (2000).
- Keisuke Oguro, Naoko Fujiwara, Kinji Asaka, Kazuo Onishi and Shingo Sewa, "Polymer Electrolyte Actuator with Gold Electrodes," *Proc. SPIE*, **3669**, 64-71 (1999).
- Yoseph Bar-Cohen, Stewart Sherrit, and Shyh-Shiuh Lih, "Characterization of the Electromechanical Properties of EAP Materials," *Proc. SPIE*, **4329**, 319-327 (2001).
- Xiaoqi Bao, Yoseph Bar-Cohen, and Shyh-Shiuh Lih, "Measurements and Macro Models of Ionomeric Polymer-metal Composites (IPMC)," *Proc. SPIE*, **4695**, 220-227 (2002).
- William Y. Hsu and Timothy D. Gierke, "Ion Transport and Clustering in Nafion Perfluorinated Membranes," *J. Membrane Science*, **13**, 307-326 (1983).
- Kinji Asaka, Naoko Fujiwara, Keisuke Oguro, Kazuo Onishi, and Shingo Sewa, "State of Water and Ionic Conductivity of Solid Polymer Electrolyte Membranes in Relation to Polymer Actuators," *J. Electroanal. Chem.*, **505**, 24-32 (2001).
- Kenneth M. Newbury and Donald J. Leo, "Electrically Induced Permanent Strain in Ionic Polymer-metal Composite Actuators," *Proc. SPIE*, **4695**, 67-77 (2002).
- Here EW_{H^+} refers to the equivalent weight of bare ionomer in H^+ -form and EW_{A^+} refers to the equivalent weight of the corresponding IPMC with cation A^+ .
- Mohsen Shahinpoor and Kwang J. Kim, "The Effect of Surface-electrode Resistance on the Performance of Ionic Polymer-metal Composite (IPMC) Artificial Muscles," *Smart Mater. Struct.*, **9**, 543-551 (2000).
- Note that the subscripts B and M for the strain and stress in Eq. (27) of Nemat-Nasser (Ref. 4) are reversed due to typographical errors. The final result, Eq. (30), corresponding to Eq. (A14) is however correct.